

## Synthesis, antioxidant activity and docking studies of 2-(aroylmethylthio)imidazoles and 3-arylimidazo[2,1-*b*]thiazoles

Nataliia Slyvka<sup>a\*</sup>, Lesya Saliyeva<sup>a</sup>, Serhiy Suprunovich<sup>a</sup>, Mariia Kizym<sup>a</sup>, Victor Tkachuk<sup>b</sup> and Mykhailo Vovk<sup>b</sup>

<sup>a</sup>Department of Organic and Pharmaceutical Chemistry, Lesya Ukrainka Volyn National University, Voli Ave. 13, Lutsk 43025, Ukraine

<sup>b</sup>Department of Functional Heterocyclic Systems, Institute of Organic Chemistry of National Academy of Sciences of Ukraine, Academician Kuharya St. 5, Kyiv 02660, Ukraine

### CHRONICLE

#### Article history:

Received April 25, 2025

Received in revised form

June 27, 2025

Accepted December 3, 2025

Available online

December 3, 2025

#### Keywords:

Imidazo[2,1-*b*][1,3]thiazole

Polyphosphoric acid

Electrophilic intramolecular

cyclization

Antioxidant activity

### ABSTRACT

A convenient method has been developed for the synthesis of a focused library of eight 3-arylimidazo[2,1-*b*][1,3]thiazoles **4a–h**, seven of which have been obtained for the first time. The approach is based on the cyclization of 2-(aroylmethylthio)imidazoles **3a–h** under the action of polyphosphoric acid. The structure of the intermediate derivatives of thioimidazoles **3a–h** and the imidazothiazoles **4a–h** thus obtained was characterized using <sup>1</sup>H, <sup>13</sup>C NMR spectra and LC-MS. Testing all obtained compounds for antioxidant activity showed that 2-[(1*H*-imidazol-2-yl)thio]-1-arylethanones **3a–h** exhibit a higher ability to inhibit DPPH radicals compared to their cyclic analogues, 3-arylimidazo[2,1-*b*]thiazoles **4a–h**. The highest antioxidant activity was demonstrated by compound **3b** (I = 96.3%), which also showed high binding affinity to the Kelch domain of the Keap1 protein in docking studies.

© 2026 by the authors; licensee Growing Science, Canada.

## 1. Introduction

Over the past few decades, condensed heterocyclic compounds have become an integral part of fundamental research in the fields of organic, medicinal, and pharmaceutical chemistry. Due to their unique structural features and a wide range of biological activities, they are promising candidates for the creation of new drugs, pesticides, and other biologically active substances. One of the most promising approaches to creating innovative therapeutic agents is the combination of structural elements from several pharmacologically potent fragments. This approach contributes to the enhancement of the biological effect, increased selectivity of interaction with biotargets, and reduced side effects (See Fig. 1).

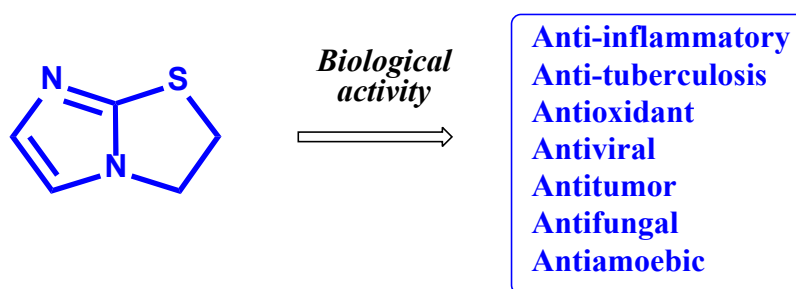


Fig. 1. Pharmacological profile of imidazo[2,1-*b*][1,3]thiazole scaffold.

\* Corresponding author Tel.:

E-mail address [slyvka.natalia@vnu.edu.ua](mailto:slyvka.natalia@vnu.edu.ua) (N. Slyvka)

© 2026 by the authors; licensee Growing Science, Canada

doi: 10.5267/j.ccl.2025.12.002

An important role in the design of biorelevant compounds is played by consensed azole systems and their hydrogenated and condensed derivatives, which are effective molecular platforms for the creation of new molecules with improved physicochemical and biological properties<sup>1-5</sup>. In modern drug development strategies, key positions in the array of azole heterocycles are occupied by structures that contain the imidazo[2,1-*b*]thiazole skeleton and exhibit anti-inflammatory<sup>6,7</sup> anti-tuberculosis<sup>8</sup>, antioxidant<sup>9</sup>, antimicrobial<sup>10</sup>, antiviral<sup>11</sup>, antitumor<sup>12,13</sup> and antiamebic<sup>14</sup> effects.

Recently<sup>15</sup> we developed an efficient method for obtaining a series of hydrogenated analogues of imidazothiazoles, new 3-aryl-5,6-dihydroimidazo[2,1-*b*][1,3]thiazoles, which demonstrated the promise of the search for bioactive substances by the annelation of the thiazole nucleus to the imidazolidine ring. Indeed, the synthesized hydrogenated imidazo-thiazole compounds showed greater antibacterial and fairly high antifungal antioxidant activity.<sup>15</sup> It is likely that the obtained result is largely due to the biophoric potential of the arylidene-functionalized imidazo-thiazole scaffold, which was formed during the synthesis process.<sup>16,17</sup> The imidazo[2,1-*b*]thiazole fragment is an integral part of the molecular structure of a series of pharmacologically active compounds, e.g. anxiolytic WAY-181187 (SAX-187) **I**,<sup>18</sup> which is a positive allosteric modulator of serotonin 5-HT<sub>6</sub> receptors and demonstrates promising properties in the treatment of anxiety disorders; the basic element of the structure of levamisole **II**,<sup>19</sup> anthelmintic and immunomodulatory drug; quizartinib **III**,<sup>20</sup> an anticancer drug that has shown high efficacy in the treatment of acute myeloid leukemia; an orally active anticancer drug **V**,<sup>21</sup> with selective action on vascular endothelial cells that stimulate HUVEC proliferation; and pifitrin- $\beta$  **IV**,<sup>22</sup> an anticancer agent that effectively inhibits the p53 protein, a key regulator of the cell cycle and apoptosis, with an IC<sub>50</sub> of 23 nM (**Fig. 2**).

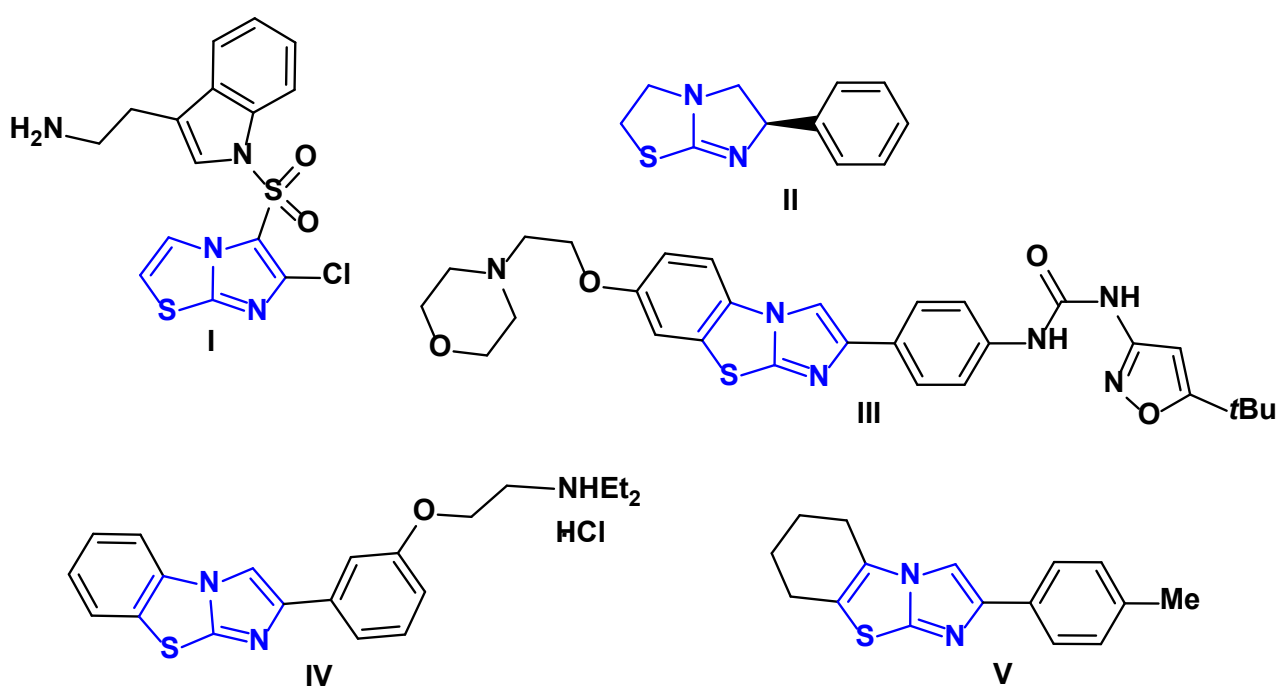


**Fig. 2.** Some examples of the bioactive compounds containing the imidazothiazole fragments (**I-V**).

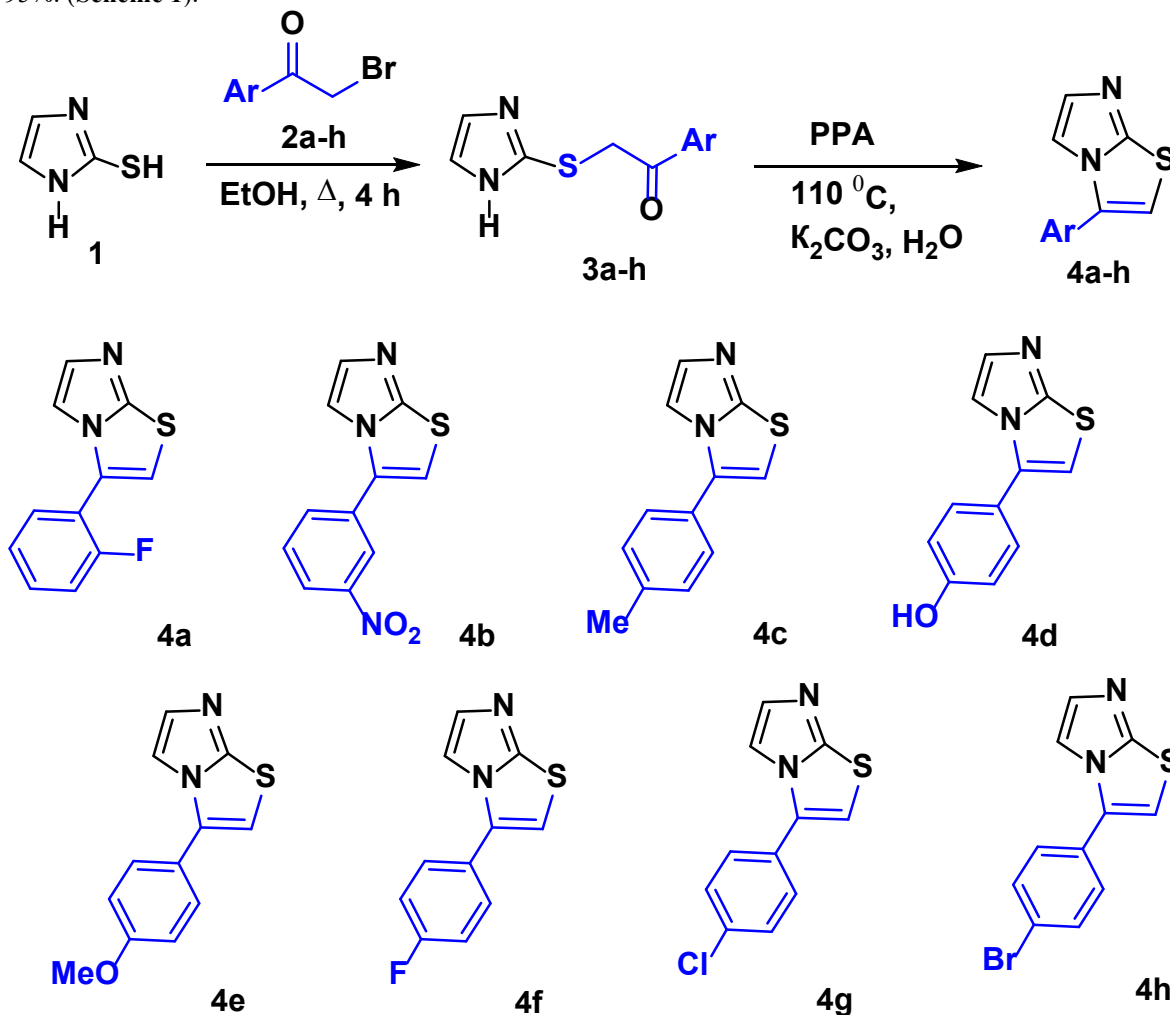
Given that the design of molecules with several pharmacophore fragments is one of the most effective approaches to the search for drug-like agents, the task of this study was to create a focused library of new 3-aryl-substituted imidazo[2,1-*b*][1,3]thiazoles and evaluate their antioxidant properties. This type of compound has previously been shown to be potential cardiogenic agents<sup>23</sup> and indoleamine 2,3-dioxygenase inhibitors<sup>17</sup>. In this context, the presented work is a continuation of our previous studies<sup>15</sup>, which concerned the synthesis and some biological properties of 3-aryl-5,6-dihydroimidazo[2,1-*b*][1,3]thiazoles. An important task was also to compare the antioxidant activity of 3-aryl-substituted imidazo[2,1-*b*][1,3]thiazoles and their synthetic precursors, 2-(aroylmethylthio)imidazoles. It is known that the structural fragment of the latter is part of highly effective inhibitors of the enzyme 11 $\beta$ -hydroxysteroid dehydrogenase type 1,<sup>24</sup> inhibitors of EGER<sup>25</sup> and cathepsin X<sup>26</sup>, as well as a number of compounds with anticancer,<sup>27</sup> antibacterial<sup>28,29</sup> and antifungal<sup>30</sup> activity.

## 2. Results and Discussion

### 2.1. Chemistry

The currently described methods for the preparation of a few 3-substituted imidazo[2,1-*b*][1,3]thiazoles are based on two main synthetic approaches, 1) annelation of the imidazole nucleus by cyclocondensation of 2-amino-1,3-thiazoles with 2-bromo-4'-bromoacetophenone<sup>31</sup> or bromoacetaldehyde dimethyl acetal<sup>32</sup>; 2) annelation of the thiazole ring to 1,3-dihydro-

2-imidazole-2-thione by interaction with 1,1-dibromoalkenes,<sup>33</sup> acetophenone<sup>34</sup> and halomethyl ketones<sup>35,36</sup>. The latter reaction includes the stages of the initial formation of S-arylmethylation products and their subsequent cyclocondensation in the environment of highly aggressive phosphoryl chloride or polyphosphoric acid (PPA)<sup>36</sup>. It is worth noting that the approach using PPA at the stage of thiazole ring formation, despite its preparative simplicity, is currently limited to the example of the synthesis of 3-(4-chloro-3-nitrophenyl)imidazo[2,1-*b*][1,3]thiazole, implemented in a single example, and has not yet gained widespread use in organic synthesis. That is why it seemed appropriate to extend it to a number of new 2-(arylmethylthio)imidazoles **3a-h**, obtained in 71-88% yields by selective alkylation of imidazoline-2-thione **1** with phenacyl bromides **2a-h** at boiling for 4 h in ethanol. It was found that compounds **3a-h**, when heated in PPA at 110 °C for 1 h, quite easily undergo intramolecular cyclization with the formation of 3-arylimidazo[2,1-*b*][1,3]thiazoles **4a-h** with yields of 78-95%. (Scheme 1).



**Scheme 1.** Synthesis of the 2-(arylmethylthio)imidazoles **3a-h** and 3-arylimidazo[2,1-*b*]thiazoles **4a-h**.

The structure of the synthesized intermediate and target compounds was confirmed by the results of <sup>1</sup>H NMR, <sup>13</sup>C NMR and LC-MS spectra measurements presented in the experimental part. Particularly, the presence in the <sup>1</sup>H NMR spectra of 2-(arylmethylthio)imidazoles **3a-h** of singlets of protons of the SCH<sub>2</sub>- group, which are identified in the interval 4.56-5.05 m.p. and singlets of protons H-4, H-5 of the imidazole ring at 6.89-7.74 m.p., which in the case of compound **3e** overlap with protons of the aromatic substituent, is indicative. The formation of 3-aryl-substituted thiazole nucleus in compounds **4a-h** is confirmed by the presence in the <sup>1</sup>H NMR spectra of singlets of H-2 protons at 7.73-7.39 m.p. and signals of protons of the aromatic nucleus in the range 6.94-8.52 m. p., which for compounds **4a,e** overlap with signals of protons of the imidazole ring.

## 2.2. Antioxidant activity

The synthesized 2-[(1*H*-imidazol-2-yl)thio]-1-arylethanones **3a-h** and 3-arylimidazo[2,1-*b*]thiazoles **4a-h** were evaluated for their ability to inhibit DPPH radicals (1,1-diphenyl-2-picrylhydrazyl).<sup>34</sup> The DPPH radical scavenging activity by derivatives **3** and **4** was assessed at a concentration of 5 mM (methanol solution, measured after 60 min of incubation). This approach enables rapid identification of potential hit compounds with time and quantity savings. Ascorbic acid was used as a reference compound. According to the screening results, compounds **3b**, **3g**, and **4a**, **4h** showed the highest percentage of DPPH radical inhibition of 96.3%, 96.1%, and 93.6%, 77.2%, respectively (Fig. 3).

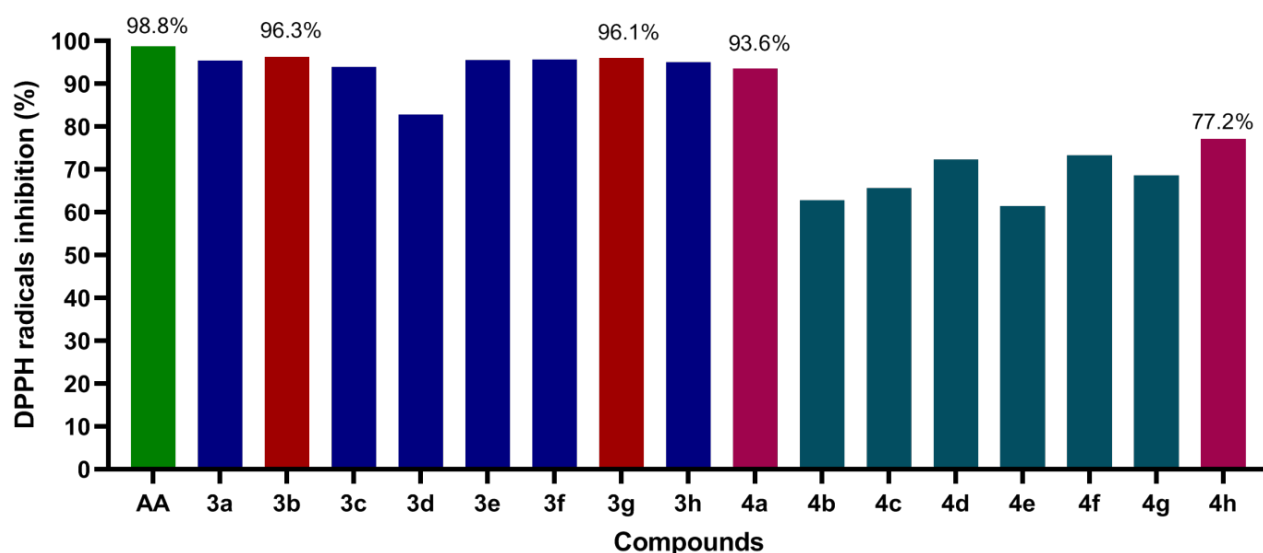
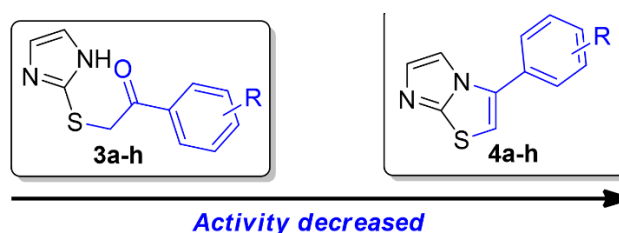


Fig. 3. The inhibition of DPPH radicals by the derivatives **3** and **4** at a 5 mM concentration.

Ascorbic acid (AA) was employed as a positive control (green). The highest activity was observed for compounds **3b**, **g** (red) and **4a**, **h** (pink).

The analysis of the structure-activity relationship demonstrated a significant influence of the structure of the studied compounds **3** and **4** on the antioxidant activity. Thus, 2-[(1*H*-imidazol-2-yl)thio]-1-arylethanones **3a-h** are characterized by higher antiradical activity than the imidazothiazoles **4a-h** derived from them. Compounds **3a-h** inhibit 82.9-96.3% of DPPH radicals, while derivatives **4a-h** inhibit 61.5-93.6% of free radicals.



### 2.3. Docking studies

The DPPH assay confirms a compound's direct antioxidant ability to quench free radicals, yet it doesn't reveal the molecular mechanism within a cell. To bridge this gap, we perform molecular docking targeting the Keap1 protein, the cell's master regulator of the antioxidant defense system. Keap1 normally acts as a negative regulator, binding to the Nrf2 transcription factor and tagging it for destruction. By choosing the Keap1 Kelch domain as the target, we focus on the critical region where the repressive Keap1–Nrf2 protein-protein interaction takes place. High-affinity binding of a compound to this domain suggests it can act as a disruptor of this interaction. This disruption would release the Nrf2 factor, allowing it to translocate to the nucleus and activate the expression of protective antioxidant and detoxification genes. Therefore, successful docking provides strong computational evidence that the DPPH-active compounds can induce the systemic cellular defense response, establishing a clear connection between the *in vitro* radical scavenging results and the *in vivo* potential.

To accomplish this computational strategy, specific crystal structures of the Kelch domain were required; therefore, PDB structures 5fnu, 6qmd, 4l7b, and 6zex were chosen due to their representation of the Keap1 Kelch domain bound to inhibitors, which allows for computational identification of compounds capable of disrupting Keap1–Nrf2 binding and subsequently activating the cell's crucial endogenous antioxidant defense.

The subsequent docking simulation yielded promising results for the tested compounds.

The tested compounds exhibited moderate to strong binding affinities toward the Keap1 Kelch domain (Table 1), consistent with their antioxidant activity observed in the DPPH assay. Among them, compound **3b** showed the most stable interaction across all analyzed structures (binding energy up to  $-7.6$  kcal/mol), while compound **4b** also demonstrated favorable binding. Reference ligands such as L6I and QHN confirmed the reliability of the docking protocol through high-affinity scores. Notably, other compounds also displayed strong binding potential. Compound **4b** showed a high docking

score with the 4L7B structure ( $-7.7$  kcal/mol), and compound **4d** achieved its best result with 6ZEX ( $-7.4$  kcal/mol). These findings suggest that the selected molecules may modulate Keap1–Nrf2 signaling and represent promising candidates for further investigation as potential antioxidant modulators.

**Table 1.** Vina docking score of the assessed compounds (kcal/mol)

Compounds	PDB 6qmd	PDB 4l7b	PDB 6zex	PDB 5fnu
3a	-7	-6.8	-6.7	-6.7
3b	-7.6	-7.4	-7.2	-7.4
3c	-7	-7	-6.7	-6.8
3d	-7	-7	-6.7	-6.9
3e	-7	-6.8	-6.7	-6.7
3f	-6.9	-6.9	-6.6	-6.7
3g	-6.9	-6.9	-6.6	-6.8
3h	-6.8	-6.8	-6.5	-6.7
4a	-7.1	-7.1	-7.1	-7.1
4b	-7.2	-7.7	-7.4	-7.3
4c	-6.9	-7.4	-6.8	-6.9
4d	-7.3	-7.5	-7.3	-7.4
4e	-6.8	-6.8	-6.8	-6.7
4f	-6.9	-6.8	-6.8	-6.8
4g	-6.8	-6.9	-6.8	-6.8
4h	-6.9	-6.8	-6.8	-6.8
J6N*	-8.9			
1VV*		-11.6		
QHN*			-7	
L6I				-12.3

\*Abbreviations used by Protein data bank

The receptor-ligand interactions of the most attractive compounds have been studied (Fig. 4-7). Some ligands **3b**, **4b**, and **4d** exhibited favorable interactions within the Keap1 Kelch domain binding pocket across various crystal structures. All compounds formed conventional hydrogen bonds with key amino acid residues such as Gly367, Leu365, Val606, Ser602, and Ile416, indicating strong polar interactions that help stabilize the ligand-receptor complexes.  $\pi$ -interactions were commonly observed, including  $\pi$ - $\pi$  stacking (notably with Tyr334 and Tyr572),  $\pi$ - $\sigma$ , and  $\pi$ -alkyl bonds, particularly with residues like Arg415, Ala366, and Ala556, highlighting the role of aromatic and hydrophobic contacts. Compound **3b** showed a diverse interaction profile in 6QMD, including both hydrogen bonding and multiple  $\pi$ -type interactions. Compound **4b** demonstrated strong aromatic stacking in 4L7B and hydrogen bonding in 6ZEX, while compound **4d** interacted with 5FNU through polar and hydrophobic contacts, though an unfavorable donor-donor interaction was noted near Gly367. Overall, the interaction patterns support the hypothesis that these ligands can effectively bind to the Kelch domain and potentially disrupt the Keap1–Nrf2 interaction.

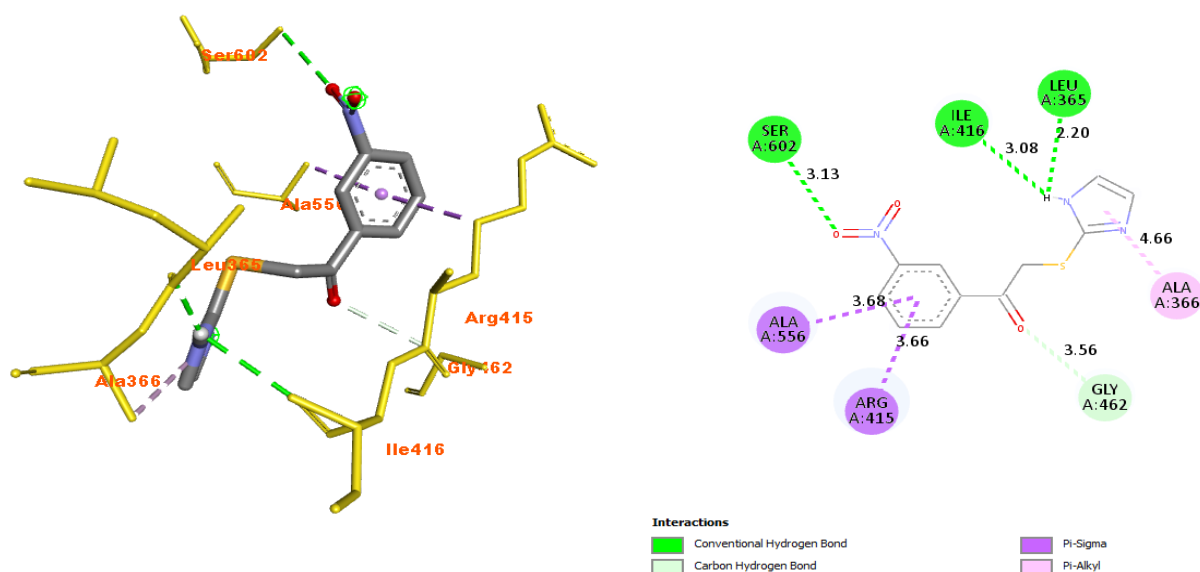


**Fig. 4.** The 3D and 2D interaction schemes of the **6qmd-3b** complex

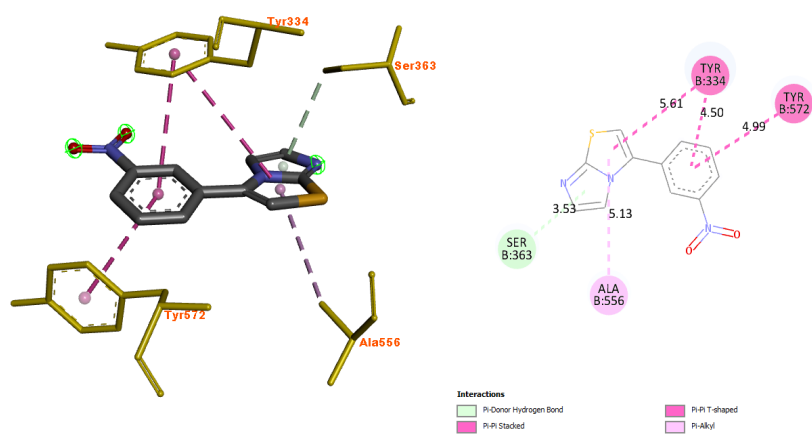


Fig. 5. The 3D and 2D interaction schemes of the **417b-4b** complex.

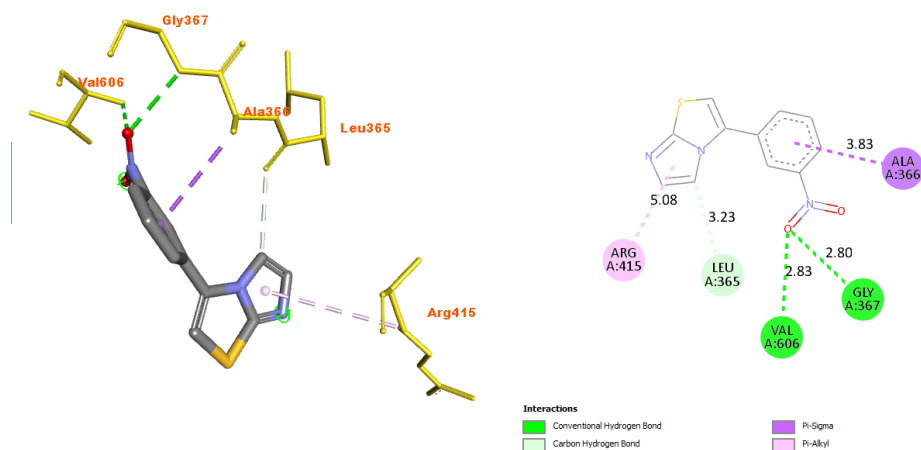


Fig. 6. The 3D and 2D interaction schemes of the **6zex-4b** complex

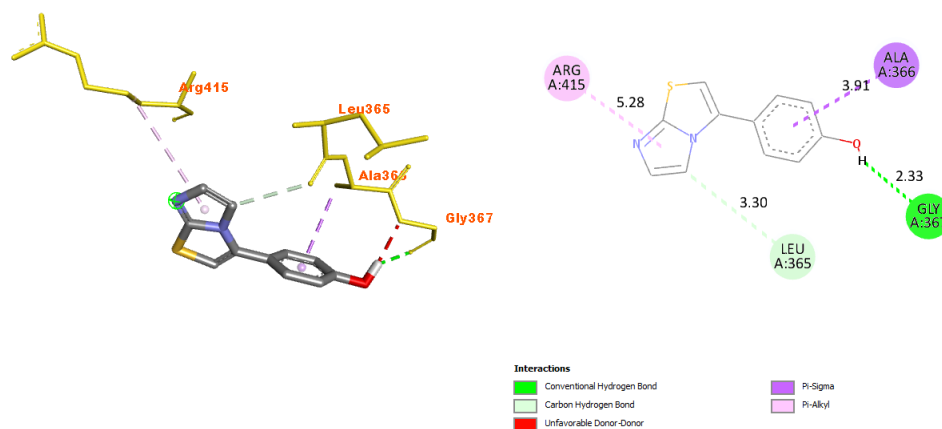


Figure 7. The 3D and 2D interaction schemes of the **5fnu-4d** complex

### 3. Conclusions

We developed a convenient method for constructing a focused library of eight 3-arylimidazo[2,1-*b*][1,3]thiazoles **4a-h**, seven of which were obtained for the first time, based on the PPA-induced intramolecular cyclization of 2-

(aroylmethylthio)imidazoles **3a–h**. The antioxidant activity of the synthesized compounds was investigated by the DPPH radical scavenging assay. It was found that 2-(aroylmethylthio)imidazoles **3a–h** exhibit a higher free radical scavenging capacity with inhibitory activity in the range of 82.9–96.3%, compared to the corresponding cyclic 3-arylimidazo[2,1-*b*][1,3]thiazoles **4a–h**, for which this indicator was 61.5–93.6%. The highest activity was shown by compound **3b**, which achieved 96.3% inhibition of DPPH radicals. Molecular docking study indicates high affinity of this compound for the Kelch domain of the Keap1 protein, indicating its potential ability to modulate the Keap1–Nrf2 signaling pathway.

## 4. Experimental

### 4.1 Chemistry

All the reagents and solvents used in the present work were of the “chemically pure” grade. No additional purification of the reactants was applied before the syntheses. Standard methods of the solvent purification were used. Melting points were measured on a Kofler bench and are uncorrected. <sup>1</sup>H NMR spectra were acquired in pulsed Fourier transform mode on a Varian VXR-400 spectrometer (400 MHz), while <sup>13</sup>C NMR spectra were acquired on a Bruker Avance DRX-500 spectrometer (126 MHz), using DMSO-*d*<sub>6</sub> as a solvent, reference: δ (TMS) = 0 ppm. Mass spectra were recorded on an Agilent LC/MSD SL chromatograph equipped with a Zorbax SB-C<sub>18</sub> column (4.6x15mm), particle size 1.8 μm (PN 82(c)75-932), solvent DMSO, electrospray ionization at atmospheric pressure. Elemental analysis was performed on a PerkinElmer 2400 CHN Analyzer. TLC monitored the individuality of the obtained compounds on Silutol UV-254 plates (eluent MeOH-CHCl<sub>3</sub>, 1:50).

**4.1.1 General procedure for the synthesis of 2-[(1*H*-Imidazol-2-yl)thio]-1-arylethanones **3a–h**.** To a suspension of 0.25 g (2.48 mmol) of imidazolidine-2-thione **1** in 10 mL of EtOH was added 2.48 mmol of K<sub>2</sub>CO<sub>3</sub> and 2.48 mmol of the corresponding phenacyl bromide **2a–h**. The reaction mixture was stirred for 48 h, then poured onto ice. The precipitate formed was filtered, recrystallized from isopropanol, and dried.

**4.1.2 2-[(1*H*-Imidazol-2-yl)thio]-1-(2-fluorophenyl)ethanone (**3a**).** Yellow solid, mp 134–135 °C; yield 71 %. <sup>1</sup>H NMR (300 MHz, DMSO-*d*<sub>6</sub>): δ 4.56 (s, 2H, CH<sub>2</sub>), 7.01 (s, 2H, H-4, H-5), 7.34–7.41 (m, 2H, Ar), 7.69 (s, 1H, Ar), 7.84 (s, 1H, Ar), 12.24 (s, 1H, NH). <sup>13</sup>C NMR (100 MHz, DMSO-*d*<sub>6</sub>): δ = 44.4 (SCH<sub>2</sub>), 117.3 (d, <sup>2</sup>J<sub>C,F</sub> = 23.0 Hz, Ar), 124.4 (d, <sup>3</sup>J<sub>C,F</sub> = 13.0 Hz, Ar), 125.3 (d, <sup>5</sup>J<sub>C,F</sub> = 3.0 Hz, Ar), 131.2 (Ar+C<sup>4</sup>+C<sup>5</sup>), 135.9 (d, <sup>4</sup>J<sub>C,F</sub> = 10.0 Hz, Ar), 138.2 (C<sup>2</sup>), 161.4 (d, <sup>1</sup>J<sub>C,F</sub> = 252.0 Hz, Ar), 192.3 (C=O). MS: m/z 237 (M + H). Anal. Calcd. for C<sub>11</sub>H<sub>9</sub>FN<sub>2</sub>OS (%): C, 55.92; H, 3.84; N, 11.86. Found: C, 56.13; H, 3.80; N, 11.69.

**4.1.3 2-[(1*H*-Imidazol-2-yl)thio]-1-(3-nitrophenyl)ethanone (**3b**).** Yellow solid, mp 125–126 °C; yield 84 %. <sup>1</sup>H NMR (300 MHz, DMSO-*d*<sub>6</sub>): δ 4.71 (s, 2H, CH<sub>2</sub>), 7.01 (s, 2H, H-4,H-5), 7.81 (t, <sup>3</sup>J = 9.0 Hz, 1H, Ar), 8.37 (d, <sup>3</sup>J = 9.0 Hz, 1H, Ar), 8.46 (d, <sup>3</sup>J = 6.0 Hz, 1H, Ar), 8.65 (s, 1H, Ar). The proton of the NH group is in exchange with water molecules of the deuteriosolvent. <sup>13</sup>C NMR (125 MHz, DMSO-*d*<sub>6</sub>): δ = 40.8 (SCH<sub>2</sub>), 123.3, 128.0 (Ar), 131.0 (Ar+C<sup>4</sup>+C<sup>5</sup>), 135.0, 137.0 (Ar), 137.8 (C<sup>2</sup>), 148.4 (Ar), 193.3 (C=O). MS: m/z 264 (M + H). Anal. Calcd. for C<sub>11</sub>H<sub>9</sub>N<sub>3</sub>O<sub>3</sub>S (%): C, 50.18; H, 3.45; N, 15.96. Found: C, 50.41; H, 3.46; N, 15.77.

**4.1.4 2-[(1*H*-Imidazol-2-yl)thio]-1-(*p*-tolyl)ethanone (**3c**).** White solid, mp 132–134 °C; yield 79 %. <sup>1</sup>H NMR (300 MHz, DMSO-*d*<sub>6</sub>): δ 2.38 (s, 3H, Me), 4.65 (s, 2H, CH<sub>2</sub>), 7.02 (s, 2H, H-4,H-5), 7.33 (d, <sup>3</sup>J = 6.0 Hz, 2H, Ar), 7.87 (d, <sup>3</sup>J = 6.0 Hz, 2H, Ar), 12.24 (s, 1H, NH). <sup>13</sup>C NMR (125 MHz, DMSO-*d*<sub>6</sub>): δ = 21.6 (Me), 40.9 (SCH<sub>2</sub>), 129.0 (Ar), 129.7 (Ar+C<sup>4</sup>+C<sup>5</sup>), 133.3 (Ar), 138.4 (C<sup>2</sup>), 144.5 (Ar), 194.0 (C=O). MS: m/z 233 (M + H). Anal. Calcd. for C<sub>12</sub>H<sub>12</sub>N<sub>2</sub>O<sub>2</sub>S (%): C, 62.04; H, 5.21; N, 12.06. Found: C, 62.27; H, 5.18; N, 12.21.

**4.1.5 2-[(1*H*-Imidazol-2-yl)thio]-1-(4-hydroxyphenyl)ethanone (**3d**).** Light yellow solid, mp 237–239 °C; yield 72 %. <sup>1</sup>H NMR (300 MHz, DMSO-*d*<sub>6</sub>): δ 5.06 (s, 2H, CH<sub>2</sub>), 6.91 (d, <sup>3</sup>J = 9.0 Hz, 2H, Ar), 7.74 (s, 2H, H-4,H-5), 7.89 (d, <sup>3</sup>J = 9.0 Hz, 2H, Ar), 10.06 (s, 1H, NH), 14.46 (s, 1H, OH). <sup>13</sup>C NMR (100 MHz, DMSO-*d*<sub>6</sub>): δ = 42.1 (SCH<sub>2</sub>), 116.0, 121.4, 126.6 (Ar), 131.7 (C<sup>4</sup>+C<sup>5</sup>), 140.6 (C<sup>2</sup>), 163.4 (Ar), 191.2 (C=O). MS: m/z 235 (M + H). Anal. Calcd. for C<sub>11</sub>H<sub>10</sub>N<sub>2</sub>O<sub>2</sub>S (%): C, 56.39; H, 4.30; N, 11.96. Found: C, 56.55; H, 4.26; N, 11.72.

**4.1.6 2-[(1*H*-Imidazol-2-yl)thio]-1-(4-methoxyphenyl)ethanone (**3e**).** White solid, mp 139–140 °C; yield 71 %. <sup>1</sup>H NMR (300 MHz, DMSO-*d*<sub>6</sub>): δ 3.85 (s, 3H, OMe), 4.62 (s, 2H, CH<sub>2</sub>), 7.03–7.08 (m, 4H, H-4,H-5+2H Ar), 7.96 (d, <sup>3</sup>J = 9.0 Hz, 2H, Ar), 12.13 (s, 1H, NH). <sup>13</sup>C NMR (125 MHz, DMSO-*d*<sub>6</sub>): δ = 40.2 (SCH<sub>2</sub>), 55.6 (OMe), 113.9, 128.2 (Ar), 130.8 (Ar+C<sup>4</sup>+C<sup>5</sup>), 138.0 (C<sup>2</sup>), 163.4 (Ar), 192.4 (C=O). MS: m/z 249 (M + H). Anal. Calcd. for C<sub>12</sub>H<sub>12</sub>N<sub>2</sub>O<sub>2</sub>S (%): C, 58.05; H, 4.87; N, 11.28. Found: C, 57.79; H, 4.83; N, 11.42.

**4.1.7 2-[(1*H*-Imidazol-2-yl)thio]-1-(4-fluorophenyl)ethanone (**3f**).** White solid, mp 147–148 °C; yield 78 %. <sup>1</sup>H NMR (300 MHz, DMSO-*d*<sub>6</sub>): δ 4.65 (s, 2H, CH<sub>2</sub>), 6.89 (s, 1H, H-4), 7.09 (s, 1H, H-5), 7.36 (d, <sup>3</sup>J = 9.0 Hz, 2H, Ar), 8.06 7.96 (d, <sup>3</sup>J = 9.0 Hz, 2H, Ar), 12.27 (s, 1H, NH). <sup>13</sup>C NMR (125 MHz, DMSO-*d*<sub>6</sub>): δ = 40.7 (SCH<sub>2</sub>), 116.2 (d, <sup>2</sup>J<sub>C,F</sub> = 21.25 Hz, Ar), 131.9 (d, <sup>3</sup>J<sub>C,F</sub> = 7.5 Hz, Ar+C<sup>4</sup>+C<sup>5</sup>), 132.5 (d, <sup>4</sup>J<sub>C,F</sub> = 3.75 Hz, Ar), 138.2 (C<sup>2</sup>), 165.6 (d, <sup>1</sup>J<sub>C,F</sub> = 251.25 Hz, Ar), 193.2

(C=O). MS:  $m/z$  237 (M + H). Anal. Calcd. for  $C_{11}H_9FN_2OS$  (%): C, 55.92; H, 3.84; N, 11.86. Found: C, 56.17; H, 3.86; N, 12.03.

**4.1.8 2-[(1*H*-Imidazol-2-yl)thio]-1-(4-chlorophenyl)ethanone (3g).** Light yellow solid, mp 130-131 °C; yield 83 %.  $^1H$  NMR (300 MHz, DMSO- $d_6$ ):  $\delta$  4.65 (s, 2H, CH<sub>2</sub>), 7.02 (s, 2H, H-4,H-5), 7.60 (d,  $^3J = 9.0$  Hz, 2H, Ar), 7.98 (d,  $^3J = 6.0$  Hz, 2H, Ar), 12.29 (s, 1H, NH).  $^{13}C$  NMR (150 MHz, DMSO- $d_6$ ):  $\delta$  = 40.8 (SCH<sub>2</sub>), 129.3 (Ar), 130.8 (Ar+C<sup>4</sup>+C<sup>5</sup>), 134.5, 138.1 (Ar), 138.9 (C<sup>2</sup>), 193.6 (C=O). MS:  $m/z$  253 (M + H). Anal. Calcd. for  $C_{11}H_9ClN_2OS$  (%): C, 52.28; H, 3.59; N, 11.08. Found: C, 52.02; H, 3.61; N, 11.22.

**4.1.9 2-[(1*H*-Imidazol-2-yl)thio]-1-(4-bromophenyl)ethanone (3h).** White solid, mp 115-116 °C; 85 %.  $^1H$  NMR (300 MHz, DMSO- $d_6$ ):  $\delta$  4.63 (s, 2H, CH<sub>2</sub>), 7.01 (s, 2H, H-4,H-5), 7.74 (d,  $^3J = 9.0$  Hz, 2H, Ar), 7.90 (d,  $^3J = 9.0$  Hz, 2H, Ar), 12.27 (s, 1H, NH).  $^{13}C$  NMR (150 MHz, DMSO- $d_6$ ):  $\delta$  = 40.7 (SCH<sub>2</sub>), 128.1 (Ar), 130.9 (Ar+C<sup>4</sup>+C<sup>5</sup>), 132.2, 134.8 (Ar), 138.1 (C<sup>2</sup>), 193.9 (C=O). MS:  $m/z$  298 (M + H). Anal. Calcd. for  $C_{11}H_9BrN_2OS$  (%): C, 44.46; H, 3.05; N, 9.43. Found: C, 44.70; H, 3.01; N, 9.28.

**4.1.10 General procedure for the synthesis of 3-arylimidazo[2,1-*b*]thiazoles 4a-h.** To the mixture of 10 g of H<sub>3</sub>PO<sub>4</sub> and 10 g of P<sub>2</sub>O<sub>5</sub> were added 2.0 mmol of the corresponding 2-[(1*H*-imidazol-2-yl)thio]-1-arylethanone **3a-h** with stirring. The reaction mixture was heated for 1 h at 110 °C, left overnight, and then poured into 50 g of ice. It was neutralized with a saturated K<sub>2</sub>CO<sub>3</sub> solution, extracted with CHCl<sub>3</sub> (3 × 10 mL), and evaporated. The residue was purified by recrystallization from isopropanol (compound **4a-d,f-h**) or by chromatography on silica gel (compound **4e**).

**4.1.11 3-(2-Fluorophenyl)imidazo[2,1-*b*]thiazole (4a).** Light brown solid, mp 76-78 °C; yield 58 %.  $^1H$  NMR (300 MHz, DMSO- $d_6$ ):  $\delta$  7.32 (s, 1H, H-2), 7.38-7.46 (m, 2H, Ar), 7.49 (s, 1H, H-6), 7.58-7.65 (m, 1H, Ar), 7.69-7.77 (m, 2H, Ar+H-5).  $^{13}C$  NMR (125 MHz, CDCl<sub>3</sub>):  $\delta$  = 111.0 (d,  $^5J_{C,F} = 3.75$  Hz, C<sup>2</sup>), 111.9 (C<sup>5</sup>), 116.2 (d,  $^2J_{C,F} = 21.25$  Hz, Ar), 117.3 (d,  $^3J_{C,F} = 13.75$  Hz, Ar), 124.3 (d,  $^5J_{C,F} = 3.75$  Hz, Ar), 126.0 (C<sup>6</sup>), 129.1 (d,  $^6J_{C,F} = 2.5$  Hz, Ar), 130.9 (d,  $^4J_{C,F} = 8.75$  Hz, C<sup>3</sup>), 134.1 (Ar), 148.8 (C<sup>7a</sup>), 159.2 (d,  $^1J_{C,F} = 250.0$  Hz, Ar). MS:  $m/z$  219 (M + H). Anal. Calcd. for  $C_{11}H_7FN_2S$  (%): C, 60.54; H, 3.23; N, 12.84. Found: C, 60.79; H, 3.20; N, 13.02.

**4.1.12 3-(3-Nitrophenyl)imidazo[2,1-*b*]thiazole (4b).** Brown solid, mp 195-197 °C; yield 62 %.  $^1H$  NMR (300 MHz, DMSO- $d_6$ ): 7.39 (s, 1H, H-2), 7.77 (s, 1H, H-6), 7.85 (t,  $^3J = 9.0$  Hz, 1H, Ar), 8.06 (s, 1H, H-5), 8.23 (d,  $^3J = 9.0$  Hz, 1H, Ar), 8.34 (d,  $^3J = 9.0$  Hz, 1H, Ar), 8.52 (s, 1H, Ar).  $^{13}C$  NMR (150 MHz, DMSO- $d_6$ ):  $\delta$  = 112.8 (C<sup>2</sup>), 113.2 (C<sup>5</sup>), 121.9 (Ar), 124.4 (C<sup>6</sup>), 130.0 (Ar), 131.1 (C<sup>3</sup>), 134.4, 133.3, 135.3, 148.8 (Ar), 149.2 (C<sup>7a</sup>). MS:  $m/z$  246 (M + H). Anal. Calcd. for  $C_{11}H_7N_3O_2S$  (%): C, 53.87; H, 2.88; N, 17.13. Found: C, 53.09; H, 2.85; N, 17.30.

**4.1.13 3-(*p*-Tolyl)imidazo[2,1-*b*]thiazole (4c).** Orange solid, mp 71-73 °C; yield 65 %.  $^1H$  NMR (300 MHz, CDCl<sub>3</sub>):  $\delta$  2.43 (s, 3H, Me), 6.73 (s, 1H, H-2), 7.31 (d,  $^3J = 6.0$  Hz, 2H, Ar), 7.37 (s, 1H, H-6), 7.51 (d,  $^3J = 6.0$  Hz, 2H, Ar), 7.61 (s, 1H, H-5).  $^{13}C$  NMR (125 MHz, CDCl<sub>3</sub>):  $\delta$  = 20.8 (Me), 107.3 (C<sup>2</sup>), 111.3 (C<sup>5</sup>), 126.2, 126.7 (Ar), 129.4 (C<sup>6</sup>), 132.1 (C<sup>3</sup>), 134.2, 139.2 (Ar), 149.3 (C<sup>7a</sup>). MS:  $m/z$  215 (M + H). Anal. Calcd. for  $C_{10}H_{12}N_2S$  (%): C, 67.26; H, 4.70; N, 13.07. Found: C, 67.53; H, 4.68; N, 12.81.

**4.1.14 4-(Imidazo[2,1-*b*]thiazol-3-yl)phenol (4d).** Brown solid, mp 245-247 °C; yield 78 %.  $^1H$  NMR (300 MHz, DMSO- $d_6$ ):  $\delta$  6.94 (d,  $^3J = 9.0$  Hz, 2H, Ar), 7.23 (s, 1H, H-2), 7.32 (s, 1H, H-6), 7.57 (d,  $^3J = 6.0$  Hz, 2H, Ar), 7.89 (s, 1H, H-5). The proton of the OH group is in exchange with water molecules of the deuteriosolvent.  $^{13}C$  NMR (100 MHz, DMSO- $d_6$ ):  $\delta$  = 107.6 (C<sup>2</sup>), 113.1 (C<sup>5</sup>), 116.5, 120.5 (Ar), 128.6 (C<sup>6</sup>), 132.4 (C<sup>3</sup>), 134.9 (Ar), 149.1 (C<sup>7a</sup>), 159.1 (Ar). MS:  $m/z$  217 (M + H). Anal. Calcd. for  $C_{11}H_8N_2OS$  (%): C, 61.09; H, 3.73; N, 12.95. Found: C, 61.34; H, 3.70; N, 13.09.

**4.1.15 3-(4-Methoxyphenyl)imidazo[2,1-*b*]thiazole (4e).** Thick oil, yield 77 %.  $^1H$  NMR (300 MHz, DMSO- $d_6$ ):  $\delta$  3.86 (s, 3H, OMe), 6.66 (s, 1H, H-2), 7.01 (d,  $^3J = 9.0$  Hz, 2H, Ar), 7.36 (s, 1H, H-6), 7.52-7.57 (m, 3H, Ar+H-5).  $^{13}C$  NMR (150 MHz, DMSO- $d_6$ ):  $\delta$  = 55.8 (OMe), 108.4 (C<sup>2</sup>), 113.1 (C<sup>5</sup>), 115.1, 122.2 (Ar), 128.6 (C<sup>6</sup>), 132.0 (C<sup>3</sup>), 135.0 (Ar), 149.1 (C<sup>7a</sup>), 160.5 (Ar). MS:  $m/z$  231 (M + H). Anal. Calcd. for  $C_{12}H_{10}N_2S$  (%): C, 62.59; H, 4.38; N, 12.16. Found: C, 62.85; H, 4.35; N, 12.33.

**4.1.16 3-(4-Fluorophenyl)imidazo[2,1-*b*]thiazole (4f).** Orange solid, mp 97-99 °C; yield 73 %.  $^1H$  NMR (300 MHz, CDCl<sub>3</sub>):  $\delta$  6.75 (s, 1H, H-2), 7.18-7.24 (m, 2H, Ar), 7.38 (s, 1H, H-6), 7.56-7.61 (m, 3H, Ar+H-5).  $^{13}C$  NMR (150 MHz, DMSO- $d_6$ ):  $\delta$  = 110.2 (C<sup>2</sup>), 113.1 (C<sup>5</sup>), 116.7 (d,  $^2J_{C,F} = 22.5$  Hz, Ar), 126.3 (C<sup>6</sup>), 129.5 (d,  $^3J_{C,F} = 9.0$  Hz, Ar), 131.1 (C<sup>3</sup>), 135.1 (Ar), 149.1 (C<sup>7a</sup>), 163.0 (d,  $^1J_{C,F} = 246.0$  Hz, Ar). MS:  $m/z$  219 (M + H). Anal. Calcd. for  $C_{11}H_7FN_2S$  (%): C, 60.54; H, 3.23; N, 12.84. Found: C, 60.77; H, 3.25; N, 12.69.

**4.1.17 3-(4-Chlorophenyl)imidazo[2,1-*b*]thiazole (4g).** Orange solid, mp 123-125 °C; yield 74 %.  $^1H$  NMR (300 MHz, DMSO- $d_6$ ):  $\delta$  7.36 (s, 1H, H-2), 7.52 (s, 1H, H-6), 7.60 (d,  $^3J = 6.0$  Hz, 2H, Ar), 7.79 (d,  $^3J = 6.0$  Hz, 2H, Ar), 7.96 (s, 1H, H-5).  $^{13}C$  NMR (150 MHz, DMSO- $d_6$ ):  $\delta$  = 110.9 (C<sup>2</sup>), 113.2 (C<sup>5</sup>), 128.6 (Ar), 128.9 (C<sup>6</sup>), 129.8 (Ar), 131.0 (C<sup>3</sup>), 134.4, 135.1 (Ar), 149.2 (C<sup>7a</sup>). MS:  $m/z$  235 (M + H). Anal. Calcd. for  $C_{11}H_7ClN_2S$  (%): C, 56.29; H, 3.01; N, 11.94. Found: C, 56.55; H, 2.97; N, 11.80.

4.1.18 3-(4-Bromophenyl)imidazo[2,1-b]thiazole (**4h**). Orange solid, mp 119-121 °C; yield 71 %. <sup>17</sup>

#### 4.2. Antioxidant activity (DPPH assay)

Antioxidant activity of the synthesized compounds was assessed using the 2,2-diphenyl-1-picrylhydrazyl (DPPH) radical inhibition assay.<sup>37</sup> 1 ml of DPPH solution (8 mg/100 ml) was added to solutions of the tested compounds and ascorbic acid in methanol as a standard and left at room temperature in a dark place for 1 hour. The amount of absorption of radicals was determined at 517 nm relative to the standard on a UV-1800 spectrophotometer (Shimadzu, Japan). Each sample was analyzed in triplicate. The percentage of inhibition was calculated relative to the blank sample:

$$I\% = \frac{(A_{\text{blank}} - (A_{\text{sample+DPPH}} - A_{\text{sample}}))}{A_{\text{blank}}} \cdot 100\%$$

where  $A_{\text{blank}}$  is the absorption of the control reaction (includes all reagents except for the studied compound);  $A_{\text{sample+DPPH}}$  is the absorption of the studied compound after 60 min incubation with DPPH solution;  $A_{\text{sample}}$  is the absorption of the investigated compounds without DPPH solution.

#### 4.3. Molecular Docking

##### 4.3.1. Target Protein Structures

The crystal structures of the Keap1 Kelch domain were obtained from the Protein Data Bank (PDB, <https://www.rcsb.org>). The following PDB entries were selected: Keap1 bound to a small-molecule ligand (PDB ID: 6QMD)<sup>38</sup>, an inhibitor analog (PDB ID: 4L7B)<sup>39</sup>, a high-affinity ligand complex (PDB ID: 6ZEX)<sup>40</sup>, and an aromatic ligand (PDB ID: 5FNU)<sup>41</sup>. Preprocessing of the protein structures was performed using Swiss-PdbViewer (<https://spdbv.unil.ch>). Water molecules, co-crystallized ligands, and prosthetic groups were removed, and missing residues were repaired. Hydrogen atoms were added using the “reduce” tool from the ADFR suite (<https://ccsb.scripps.edu/adfr>), followed by receptor preparation via the “prepare\_receptor” script.

##### 4.3.2. Ligand Preparation

Structures of the tested ligands were drawn using Marvin Sketch (<https://www.chemaxon.com>), converted to 3D using Avogadro (<https://avogadro.cc>), and protonated at physiological pH (7.4). Energy minimization was performed using the MMFF94 force field with a convergence threshold of 10<sup>-6</sup> kcal/(Å·mol). Optimized structures were saved in MOL2 format and processed with the “prepare\_ligand” script from the ADFR suite. Reference ligands were extracted from the “Small Molecules” section of the respective PDB entries. These were similarly protonated, optimized, and prepared for docking.

##### 4.3.3. Docking procedure

Molecular docking was performed using AutoDock Vina<sup>42</sup>, selected for its balance of computational efficiency and accuracy in binding affinity prediction. Docking was performed using default parameters. The binding site was defined based on co-crystallized ligand coordinates using Discovery Studio Visualizer version 24.1 (<https://www.3ds.com/products/biovia/discovery-studio>), and the grid box dimensions were set to 30 × 30 × 30 Å. Predicted binding poses and interactions were analyzed using the same software.

## References

1. Afsina Abdulla C.M., Neetha M., Aneeja T., Anilkumar G. (2020) Synthesis and Applications of Imidazothiazoles: An Overview. *Chemistry Select*, 5(33), 10374-10386. <https://doi.org/10.1002/slct.202002842>.
2. Saliyeva L.N., Diachenko I.V., Vas'kevich R.I., Slyvka N.Yu., Vovk M.V. (2020) Imidazothiazoles and their hydrogenated analogs: methods of synthesis and biomedical potential. *Chem. Heterocycl. Comp.*, 56(11), 1394-1407. <https://doi.org/10.1007/s10593-020-02827-w>.
3. Dubina T.F., Kosarevych A.V., Kucher O.V., Sosunovych B.S., Smolii O.B., Vashchenko B.V., Grygorenko O.O. (2024) Synthesis and reactions of novel imidazo[4,5-b]pyridine building blocks. *Chem. Heterocycl. Comp.*, 60, 175–182. <https://doi.org/10.1007/s10593-024-03315-1>
4. Chaban T.I., Klenina O.V., Chaban I.H., Lelyukh M.I. (2024) Recent advances in the synthesis of thiazolo[4,5-b]pyridines. Part 1: Focus on pyridine annulation to thiazole ring (microreview). *Chem. Heterocycl. Comp.*, 60, 35–37. <https://doi.org/10.1007/s10593-024-03289-0>
5. Chulovska Z., Chaban T., Savchenko A., Komarytsya O., Dasho M., Lelyukh M., Chaban I., Ogurtsov V. (2025) Antioxidant properties of some 4-arylimino-thiazolidin-2-ones. *Curr. Chem. Lett.* 14, 365–372. <https://doi.org/10.5267/j.ccl.2024.11.001>

6. Powers L.J., Fogt S.W., Ariyan Z.S., Rippin D.J., Heilman R.D., Matthews R.J. (1981) Effect of structural change on acute toxicity and antiinflammatory activity in a series of imidazothiazoles and thiazolobenzimidazoles. *Journal of Medicinal Chemistry*, 24(5), 604–609. <https://doi.org/10.1021/jm00137a022>.
7. Kamboj P., Anjali, Imtiyaz K., Rizvi M.A., Nath V., Kumar V., Husain A., Amir M. (2024) Design, synthesis, biological assessment and molecular modeling studies of novel imidazothiazole-thiazolidinone hybrids as potential anticancer and anti-inflammatory agents. *Sci Rep.*, 14(1), 8457. <https://doi.org/10.1038/s41598-024-59063-x>.
8. Samala G., Devi P.B., Saxena S., Meda N., Yogeewari P., Sriram D. (2016) Design, synthesis and biological evaluation of imidazo[2,1-*b*]thiazole and benzo[d]imidazo[2,1-*b*]thiazole derivatives as Mycobacterium tuberculosis pantothenate synthetase inhibitors. *Bioorg. Med. Chem.*, 2016, 24, 1298-1307. <http://dx.doi.org/10.1016/j.bmc.2016.01.059>.
9. Dincel E.D., Gursoy E., Yilmaz-Ozden T., Ulusoy-Guzeldemirci N. (2020) Antioxidant activity of novel imidazo[2,1-*b*]thiazole derivatives: Design, synthesis, biological evaluation, molecular docking study and in silico ADME prediction. *Bioorg. Chem.*, 103, 104220. <https://doi.org/10.1016/j.bioorg.2020.104220>.
10. Shareef M.A., Sirisha K., Bin Sayeed I.B., Khan I., Ganapathi T., Akbar S., Kumar C.G., Kamal A., Babu B.N. (2019) Synthesis of new triazole fused imidazo[2,1-*b*]thiazole hybrids with emphasis on Staphylococcus aureus virulence factors. *Bioorg. Med. Chem. Lett.*, 29(19), 126621. <https://doi.org/10.1016/j.bmcl.2019.08.025>.
11. Wang N.Y., Xu Y., Zuo W.Q., Xiao K.J., Liu L., Zeng X.X., You X.Y., Zhang L.D., Gao C., Liu Z.H., Ye T.H., Xia Y., Xiong Y., Song X.J., Lei Q., Peng C.T., Tang H., Yang S.Y., Wei Y.Q., Yu L.T. (2015) Discovery of imidazo[2,1-*b*]thiazole HCV NS4B inhibitors exhibiting synergistic effect with other direct-acting antiviral agents. *J. Med. Chem.*, 58(6), 2764-2778. <https://doi.org/10.1021/jm501934n>.
12. Nagireddy P.K.R., Kommalapati V.K., Krishna V.S., Sriram D., Tangutur A.D., Kantevari S. (2019) Imidazo[2,1-*b*]thiazole-Coupled Natural Noscipine Derivatives was Anticancer Agents. *ACS Omega*. 21, 19382-19398. <https://doi.org/10.1021/acsomega.9b02789>.
13. Gürsoy E., Güzeldemirci N.U. (2007) Synthesis and primary cytotoxicity evaluation of new imidazo[2,1-*b*]thiazole derivatives. *European Journal of Medicinal Chemistry*, 42(3), 320–326. <https://doi.org/10.1016/j.ejmech.2006.10.012>.
14. Akbar N., El-Gamal M.I., Saeed B.Q., Oh C.-H., Abdel-Maksoud M.S., Khan N.A., Alharbi A.M., Alfahemi H., Siddiqui R. (2022) Antiamoebic Activity of Imidazothiazole Derivatives against Opportunistic Pathogen *Acanthamoeba castellanii*. *Antibiotics*, 11(9), 1183. <https://doi.org/10.3390/antibiotics11091183>.
15. Zhylko V., Saliyeva L., Slyvka N., Grozav A., Yakovychuk N., Mel'nyk D., Mel'nyk O., Litvinchuk M., Vovk M. (2025) Synthesis, antimicrobial and antioxidant activity evaluation, DFT-calculation, and docking studies of 3-aryl-5,6-dihydroimidazo[2,1-*b*][1,3]thiazoles. *Current Chemistry Letters*, 14(1), 107-118. <https://doi.org/10.5267/j.ccl.2024.9.002>.
16. Fascio M. L., Errea M. I., D'Accorso N. B. (2015) Imidazothiazole and related heterocyclic systems. Synthesis, chemical and biological properties. *European Journal of Medicinal Chemistry*, 90, 666–683. <https://doi.org/10.1016/j.ejmech.2014.12.012>.
17. Peng Y.-H., Liao F.-Y., Tseng C.-T., Kuppusamy R., Li A.-S., Chen C.-H., Fan Y.-S., Wang S.-Y., Wu M.-H., Hsueh C.-C., Chang J.-Y., Lee L.-C., Shih C., Shia K.-S., Yeh T.-K., Hung M.-S., Kuo C.-C., Song J.-S., Wu S.-Y., Ueng S.-H. (2020) Unique Sulfur-Aromatic Interactions Contribute to the Binding of Potent Imidazothiazole Indoleamine 2,3-Dioxygenase Inhibitors. *J. Med. Chem.*, 63, 1642-1659. <https://dx.doi.org/10.1021/acs.jmedchem.9b01549>.
18. Schechter L.E., Lin Q., Smith D.L., Zhang G., Shan Q., Platt B., Brandt M.R., Dawson L.A., Cole D., Bernotas R., Robichaud A., R-Lipson S., Beyer C.E. (2008) Neuropharmacological profile of novel and selective 5-HT6 receptor agonists: WAY-181187 and WAY-208466. *Neuropsychopharmacology*, 33, 1323-1335. <https://doi.org/10.1038/sj.npp.1301503>.
19. Amarouch H., Loiseau P.R., Bacha C., Caujolle R., Payard M., Loiseau P.M., Bories C., Gayral P. (1987) Imidazo[2,1-*b*]thiazoles: analogues du lévamisole. *Eur. J. Med. Chem.*, 22 (5), 463-466. [https://doi.org/10.1016/0223-5234\(87\)90037-7](https://doi.org/10.1016/0223-5234(87)90037-7).
20. Chao Q., Sprankle K.G., Grotzfeld R.M., Lai A.G., Carter T.A., A.M. Velasco, R.N. Gunawardane, M.D. Cramer, M.F. Gardner, James J., Zarrinkar P.P., Patel H.K., Bhagwat S.S. (2009) Identification of N-(5-tert-butyl-isoxazol-3-yl)-N'-{4-[7-(2-morpholin-4-yl-ethoxy)imidazo[2,1-*b*][1,3]-benzothiazol-2-yl]phenyl}urea dihydrochloride (AC220), a uniquely potent, selective, and efficacious FMS-like tyrosine kinase-3 (FLT3) inhibitor. *J. Med. Chem.*, 52, 7808-7816. <https://doi.org/10.1021/jm9007533>.
21. Amino N., Ideyama Y., Yamano M., Kuromitsu S., Tajinda K., Samizu K., Matsuhisa A., Kudoh M., Shibasaki M. (2006) YM-201627: An orally active antitumour agent with selective inhibition of vascular endothelial cell proliferation. *Cancer Lett.*, 238, 119-127. <https://doi.org/10.1016/j.canlet.2005.06.037>.
22. Pozzo E.D., Pietra V.L., Cosimelli B., Settimo F.D., Giacomelli C., Marinelli L., Martini C., Novellino E., Taliani S., Greco G. (2014) p53 Functional Inhibitors Behaving Like Pifithrin- $\beta$  Counteract the Alzheimer Peptide Non- $\beta$ -amyloid Component Effects in Human SH-SY5Y Cells. *ACS Chem. Neurosci.*, 5, 390–399. <https://doi.org/10.1021/cn4002208>.

23. [Güngör T., Fouquet A., Teulon J.M., Provost D., Cazes M., Cloarec A. \(1992\) Cardiotonic agents. Synthesis and cardiovascular properties of novel 2-arylbenzimidazoles and azabenzimidazoles. \*J. Med. Chem.\*, 35, 4455–4463. <https://doi.org/10.1021/jm00101a024>.](#)
24. Su X., Vicker N., Thomas M.P., Pradaux-Caggiano F., Halem H., Culler M.D., [Potter B.V.L. \(2011\) Discovery of Adamantyl Heterocyclic Ketones as Potent 11 \$\beta\$ -Hydroxysteroid Dehydrogenase Type 1 Inhibitors. \*Chem. Med. Chem.\*, 6\(8\), 1439-1451. <https://doi.org/10.1002/cmdc.201100144>.](#)
25. Castelli R., Bozza N., Cavazzoni A., Bonelli M., Vacondio F., Ferlenghi F., Callegari D., Silva C., Rivara S., Lodola A., Digiacomio G., Fumarola C., Alfieri R., Petronini P.G., Mor M. (2019) Balancing reactivity and antitumor activity: heteroarylthioacetamide derivatives as potent and time-dependent inhibitors of EGFR. *Eur. J. Med. Chem.*, 162, 507-524. <https://doi.org/10.1016/j.ejmech.2018.11.029>.
26. Fonović U.P., Knez D., Hrast M., Zidar N., Proj M., Gobec S., Kos J. (2020) Structure-activity relationships of triazole-benzodioxine inhibitors of cathepsin X. *Eur. J. Med. Chem.*, 193, 112218. <https://doi.org/10.1016/j.ejmech.2020.112218>.
27. Khazir J., Riley D.L., Chashoo G., Mir B.A., Liles D., Islam M.A., Singh S.K., Vishwakarma R.A., Pilcher L.A. (2015) Design, synthesis and anticancer activity of Michael-type thiol adducts of  $\alpha$ -santonin analogue with exocyclic methylene. *Eur. J. Med. Chem.*, 101, 769-779. <https://doi.org/10.1016/j.ejmech.2015.07.022>.
28. Li F.F., Zhao W.H., Tangadanchu V.K.R., Meng J.P., Zhou C.H. (2022) Discovery of novel phenylhydrazone-based oxindole-thiazoles as potent antibacterial agents toward *Pseudomonas aeruginosa*. *Eur. J. Med. Chem.*, 239, 114521. <https://doi.org/10.1016/j.ejmech.2022.114521>.
29. Hu Y., Hu S., Pan G., Wu D., Wang T., Yu C., Ansari M.F., Bheemanaboina R.R.Y., Cheng Y., Bai L., Zhou C., Zhang J. (2021) Potential antibacterial ethanol-bridged purineazole hybrids as dual-targeting inhibitors of MRSA. *Bioorg. Chem.*, 114, 105096. <https://doi.org/10.1016/j.bioorg.2021.105096>.
30. Özdemir A., Sever B., Altıntop M.D. (2019) New benzodioxole-based pyrazoline derivatives: Synthesis and anticandidal, in silico ADME, molecular docking studies. *Drug. Design and Discovery*, 16(1), 82-92. <https://doi.org/10.2174/1570180815666180326152726>.
31. Ulusoy N., Kiraz M., Kucukbasmaci O. (2002) New 6-(4-Bromophenyl)imidazo[2,1-b]thiazole Derivatives: Synthesis and Antimicrobial Activity. *Monatsh. Chem.*, 133(10), 1305-1315. <https://doi.org/10.1007/s007060200108>.
32. Peng Y.H., Liao F.Y., Tseng C.T., Kuppasamy R., Li A.S., Chen C.H., Fan Y.S., Wang S.Y., Wu M.H., Hsueh C.C., Chang J.Y., Lee L.C., Shih C., Shia K.S., Yeh T.K., Hung M.S., Kuo C.C., Song J.S., Wu S.Y., Ueng S.H. (2020) [Correction to Unique Sulfur-Aromatic Interactions Contribute to the Binding of Potent Imidazothiazole Indoleamine 2,3-Dioxygenase Inhibitors. \*J. Med. Chem.\*, 63\(4\), 1642-1659. <https://doi.org/10.1021/acs.jmedchem.0c00966>.](#)
33. Xu H., Zhang Y., Huang J., Chen, W. (2010) Copper-catalyzed synthesis of N-fused heterocycles through regioselective 1,2-aminothioloation of 1,1-dibromoalkenes. *Organic Letters*, 12(16), 3704-3707. <https://doi.org/10.1021/ol101563f>.
34. Zhao J., Xiao Q., Chen J., Xu J. (2020) Metal-Free Synthesis of Imidazo [2, 1-b] thiazoles from Thioimidazoles and Ketones Mediated by Selectfluor. *European Journal of Organic Chemistry*, 32, 5201-5206. <https://doi.org/10.1002/ejoc.202000815>.
35. Mazur I.A., Kochergin P.M. (1970) Studies on the imidazole series. *Chem. Het. Compd.*, 6(4), 474-476. <https://doi.org/10.1007/bf00478395>.
36. Gungor T., Fouquet A., Teulon J.M., Provost D., Cazes M., Cloarec A. (1992) Cardiotonic agents. Synthesis and cardiovascular properties of novel 2-arylbenzimidazoles and azabenzimidazoles. *J. Med. Chem.*, 35(23), 4455-4463. <https://doi.org/10.1021/jm00101a024>.
37. Brand-Williams W., Cuvelier M.E., Berset C. (1995) Use of a free radical method to evaluate antioxidant activity. *LWT-Food Science and Technology*, 28 (1), 25-30. [https://doi.org/10.1016/S0023-6438\(95\)80008-5](https://doi.org/10.1016/S0023-6438(95)80008-5).
38. Heightman T.D., Callahan J.F., Chiarparin E., Coyle J.E., Griffiths-Jones C., Lakdawala A.S., McMenamin R., Mortenson P.N., Norton D., Peakman T.M., Rich S.J., Richardson C., Rumsey W.L., Sanchez Y., Saxty G., Willems H.M.G., Wolfe L.I., Woolford A.J.-A., Wu Z., Yan H., Kerns J.K., Davies T.G. (2019) Structure–Activity and Structure–Conformation Relationships of Aryl Propionic Acid Inhibitors of the Kelch-like ECH-Associated Protein 1/Nuclear Factor Erythroid 2-Related Factor 2 (KEAP1/NRF2) Protein–Protein Interaction. *J. Med. Chem.*, 62, 9. 4683–4702. <https://doi.org/10.1021/acs.jmedchem.9b00279>.
39. Jnoff E., Albrecht C., Barker J. J., Barker O., Beaumont E., Bromidge S., Brookfield F., Brooks M., Bubert C., Ceska T., Corden V., Dawson G., Duclos S., Fryatt T., Genicot C., Jigorel E., Kwong J., Maghames R., Mushi I., Pike R., Sands Z. A., Smith M. A., Stimson C. C., Courade J.-P. Binding (2014) Mode and Structure–Activity Relationships around Direct Inhibitors of the Nrf2–Keap1 Complex. *Chem. Med. Chem.*, 9(4), 699–705. <https://doi.org/10.1002/cmdc.201300525>.
40. Pallesen J.S., Narayanan D., Tran K.T., Solbak S.M.Ø., Marseglia G., Sørensen L.M.E., Høj L.J., Munafò F., Carmona R.M.C., Garcia A.D., Desu H.L., Brambilla R., Johansen T.N., Popowicz G.M., Sattler M., Gajhede M., Bach A. (2021) Deconstructing Noncovalent Kelch-like ECH-Associated Protein 1 (Keap1) Inhibitors into Fragments to Reconstruct New Potent Compounds. *J. Med. Chem.*, 64(8), 4623–4661. <https://doi.org/10.1021/acs.jmedchem.0c02094>.

41. Davies T.G., Wixted W.E., Coyle J.E., Griffiths-Jones C., Hearn K., McMenamin R., Norton D., Rich S.J., Richardson C., Saxty G., Willems H.M.G., Woolford A.J.-A., Cottom J.E., Kou J.-P., Yonchuk J.G., Feldser H.G., Sanchez Y., Foley J.P., Bolognese B.J., Logan G., Podolin P.L., Yan H., Callahan J.F., Heightman T.D., Kerns J.K. (2016) Monoacidic Inhibitors of the Kelch-like ECH-Associated Protein 1: Nuclear Factor Erythroid 2-Related Factor 2 (KEAP1:NRF2) Protein–Protein Interaction with High Cell Potency Identified by Fragment-Based Discovery. *J. Med. Chem.*, 59(8), 3991–4006. <https://doi.org/10.1021/acs.jmedchem.6b00228>.
42. Eberhardt J., Santos-Martins D., Tillack A.F., Forli S. (2016) AutoDock Vina 1.2.0: New Docking Methods, Expanded Force Field, and Python Bindings. *J. Chem. Inf. Model.*, 61, 3891–3898. <https://doi.org/10.1021/acs.jcim.1c00203>.



© 2026 by the authors; licensee Growing Science, Canada. This is an open access article distributed under the terms and conditions of the Creative Commons Attribution (CC-BY) license (<http://creativecommons.org/licenses/by/4.0/>).